Effect of interface on epitaxy and magnetism in h-RFeO$_3$/Fe$_3$O$_4$/Al$_2$O$_3$ films (R = Lu, Yb)

Xiaozhe Zhang[1,2]**, Yuewei Yin**[2]**, Sen Yang**[1]**, Zhimao Yang**[1,4]
and Xiaoshan Xu[2,3,4,5]

[1] School of Science, MOE Key Laboratory for Nonequilibrium Synthesis and Modulation of Condensed Matter, Xi'an Jiaotong University, Xi'an 710049, People's Republic of China
[2] Department of Physics and Astronomy, University of Nebraska, Lincoln, NE 68588, United States of America
[3] Nebraska Center for Materials and Nanoscience, University of Nebraska, Lincoln, NE 68588, United States of America

E-mail: zmyang@xjtu.edu.cn and xiaoshan.xu@unl.edu

CrossMark

Abstract

We have carried out the growth of h-RFeO$_3$ (0 0 1) (R = Lu, Yb) thin films on Fe$_3$O$_4$ (1 1 1)/Al$_2$O$_3$ (0 0 1) substrates, and studied the effect of the h-RFeO$_3$ (0 0 1)/Fe$_3$O$_4$ (1 1 1) interfaces on the epitaxy and magnetism. The observed epitaxial relations between h-RFeO$_3$ and Fe$_3$O$_4$ indicate an unusual matching of Fe sub-lattices rather than a matching of O sub-lattices. The out-of-plane direction was found to be the easy magnetic axis for h-YbFeO$_3$ (0 0 1) but the hard axis for Fe$_3$O$_4$ (1 1 1) in the h-YbFeO$_3$ (0 0 1)/Fe$_3$O$_4$ (1 1 1)/Al$_2$O$_3$ (0 0 1) films, suggesting a perpendicular magnetic alignment at the h-YbFeO$_3$ (0 0 1)/Fe$_3$O$_4$ (1 1 1) interface. These results indicate that Fe$_3$O$_4$ (1 1 1)/Al$_2$O$_3$ (0 0 1) could be a promising substrate for epitaxial growth of h-RFeO$_3$ films of well-defined interface and for exploiting their spintronic properties.

Keywords: hexagonal ferrites, multiferroics, thin film epitaxy, magnetic anisotropy

S Supplementary material for this article is available online

(Some figures may appear in colour only in the online journal)

Introduction

Thin film epitaxy and heterostructures have been shown to be effective in exploiting the rich properties in transition metal oxides [1–3], taking advantage of their structural sensitivity and the complex electronic structures at the interface. While this is encouragingly true for the perovskite family of cubic or distorted cubic symmetries [4–6], the shortage of structurally compatible substrates and well-defined interfaces hinders the study of other families of materials (e.g. of trigonal or hexagonal symmetry) using thin film epitaxy.

Here we attack the problem of thin film epitaxy of hexagonal ferrites. Hexagonal ferrites h-RFeO$_3$ (R = Lu, Yb) simultaneous exhibit ferroelectric and weakly ferromagnetic orders [7–10]; they belong to a class of complex materials called multiferroics which are promising in compact and energy efficient information storage and processing [11, 12]. The few choices of substrates for preparing thin films of h-RFeO$_3$ include Al$_2$O$_3$ (0 0 1), yttrium stabilized zirconia or YSZ (1 1 1), and Pt (1 1 1) [8–10, 13–15]. A significant number of defects are expected at the interfaces between these substrates and films due to the larger lattice mismatch

($>5\%$), which undermines the study of the intrinsic properties of the thin films and interfaces, as well as the fabrication of devices.

We have recently demonstrated epitaxial growth of Fe_3O_4 $(1\,1\,1)$ on Al_2O_3 $(0\,0\,1)$ with high crystallinity and smooth surface of atomic terraces [16]. The in-plane lattice constant of Fe_3O_4 $(1\,1\,1)$ is 11.87 Å ($\sqrt{2}$ times the lattice constant) [16], which matches twice that of h-LuFeO$_3$ and h-YbFeO$_3$ in the basal plane (5.96 Å and 5.99 Å respectively) [7, 17] within a 1% difference. In addition, previous growth of h-LuFeO$_3$ indicates that Fe_3O_4 $(1\,1\,1)$ layers may naturally occur in the h-LuFeO$_3$ films, under the reducing environments (oxygen deficient or Fe rich) [15, 18]. Therefore, Fe_3O_4 $(1\,1\,1)$/Al_2O_3 $(0\,0\,1)$ may be a compatible substrate for h-RFeO$_3$, with well-defined interfaces due to the small lattice mismatch. In addition, the Fe_3O_4 $(1\,1\,1)$ layer can be employed as a bottom electrode for studying the effect of electric field in h-RFeO$_3$. Therefore, it is intriguing to prepare the h-RFeO$_3$ films on Fe_3O_4 $(1\,1\,1)$/Al_2O_3 $(0\,0\,1)$ and study their properties, especially multiferroicity. As a foundation of these studies, the intrinsic properties at the h-RFeO$_3$/Fe_3O_4 interface and their effect on the epitaxy and magnetism of the films are of great importance.

We have prepared h-RFeO$_3$ $(0\,0\,1)$/Fe_3O_4 $(1\,1\,1)$/Al_2O_3 $(0\,0\,1)$ films using pulsed laser deposition. The structural characterizations show that the films are epitaxial and the lattices of h-RFeO$_3$ $(0\,0\,1)$ and Fe_3O_4 $(1\,1\,1)$ do align according to their in-plane lattices. The interface appears to be critical in the epitaxial relations and the magnetic alignment between h-RFeO$_3$ and Fe_3O_4. These results demonstrate that Fe_3O_4 $(1\,1\,1)$/Al_2O_3 $(0\,0\,1)$ is a promising substrate for preparing hexagonal ferrites thin films with well-defined film-substrate interfaces.

Experimental

The h-RFeO$_3$ $(0\,0\,1)$/Fe_3O_4 $(1\,1\,1)$/Al_2O_3 $(0\,0\,1)$ films were grown using pulsed laser depositions [16, 18]. The Fe_3O_4 $(1\,1\,1)$ thin films (5–30 nm) were deposited epitaxially on Al_2O_3 $(0\,0\,1)$ substrates, as described in our previous work [16]. The h-RFeO$_3$ thin films (5–30 nm) were deposited epitaxially on top of the Fe_3O_4 $(1\,1\,1)$ thin films, in a 5 mTorr Ar environment at 750 °C with a laser fluence of ~1 J cm^{-2}, and a repetition rate of 2 Hz [9, 14, 19, 20]. The epitaxial relations between different layers in the films were studied with *in-situ* reflection high energy electron diffraction (RHEED) and *ex-situ* x-ray diffractions (XRD). The $\theta - 2\theta$ scans of x-ray diffraction were carried out using a Rigaku D/Max-B diffractometer, with a cobalt K-α source ($\lambda = 1.79$ Å). The rocking curve (ω scan), φ scan and reciprocal space mapping were studied using a Rigaku Smartlab diffractometer, with a copper K-α source ($\lambda = 1.54$ Å). The surface morphology of the films was studied using the atomic force microscopy (AFM) with a Bruker Dimension ICON. The magnetic properties of the h-RFeO$_3$ $(0\,0\,1)$/Fe_3O_4 $(1\,1\,1)$/Al_2O_3 $(0\,0\,1)$ films were studied using a superconducting quantum interference device (SQUID) magnetometer.

Results and discussion

First, we investigate the epitaxial relations of the h-RFeO$_3$/Fe_3O_4/Al_2O_3 films using structural characterization. Figure 1(a) shows the large-range $\theta - 2\theta$ scan of XRD of the h-RFeO$_3$ $(0\,0\,1)$/Fe_3O_4 $(1\,1\,1)$/Al_2O_3 $(0\,0\,1)$ films; no impurity phase is observed. The small-range scans were taken around the h-RFeO$_3$ $(0\,0\,2)$ and Fe_3O_4 $(1\,1\,1)$ peaks (figure 1(b)). The Laue oscillations indicate that these films have flat surfaces [7], which is consistent with the surface roughness (<1 nm) demonstrated by AFM (see the supplementary material[6] (stacks.iop.org/JPhysCM/29/164001/mmedia)). The φ scans of these films indicate that the Fe_3O_4 $(1\,1\,1)$ and h-RFeO$_3$ $(0\,0\,1)$ layers are indeed epitaxial on the Al_2O_3 $(0\,0\,1)$ substrates (see supplementary materials). Lattice constants of the h-RFeO$_3$ layers were measured using reciprocal space mapping (RSM) (see the supplementary material); the results show that for h-LuFeO$_3$, $a = 5.963$ Å, $c = 11.92$ Å and for h-YbFeO$_3$, $a = 6.021$ Å, $c = 12.07$ Å, in agreement with the previous measurements [7, 17].

The RHEED patterns obtained on different layers reveal their epitaxial relations. As shown in figure 2, two directions of incident electron beams that are perpendicular to each other (Al_2O_3 $\langle 1\,2\,0 \rangle$ and Al_2O_3 $\langle 1\,0\,0 \rangle$) were used. The RHEED patterns of all the layers (Al_2O_3, Fe_3O_4, h-LuFeO$_3$, and h-YbFeO$_3$) are in accord with in-plane triangular lattices, suggesting a relation Al_2O_3 $(0\,0\,1)$//Fe_3O_4 $(1\,1\,1)$//h-RFeO$_3$ $(0\,0\,1)$. Using the lattice constant of Al_2O_3 as the calibration, one can estimate the lattice constants of the epilayers: $a = 8.31 \pm 0.08$ Å for Fe_3O_4, $a = 5.92 \pm 0.06$ Å for h-LuFeO$_3$, and $a = 6.02 \pm 0.06$ Å for h-YbFeO$_3$, in line with values found in the XRD measurements.

The in-plane epitaxial relation Al_2O_3 $\langle 1\,0\,0 \rangle$//Fe_3O_4 $\langle -2\,1\,1 \rangle$//h-RFeO$_3$ $\langle 1\,-1\,0 \rangle$ can be extracted from the RHEED pattern (figure 2), as well as from the XRD φ scan (see the supplementary material). Previously, it was found that when h-LuFeO$_3$ was deposited directed on the Al_2O_3 $(0\,0\,1)$ substrates, the in-plane epitaxial relation was Al_2O_3 $\langle 0\,0\,1 \rangle$ // h-LuFeO$_3$ $\langle 0\,0\,1 \rangle$, which is different from the relation found in the h-RFeO$_3$ $(0\,0\,1)$/Fe_3O_4 $(1\,1\,1)$/Al_2O_3 $(0\,0\,1)$ films here. Obviously, this difference comes from the peculiar in-plane epitaxial relation between Fe_3O_4 $(1\,1\,1)$ and Al_2O_3 $(0\,0\,1)$ layers, and that between Fe_3O_4 $(1\,1\,1)$ and h-RFeO$_3$ $(0\,0\,1)$ layers.

As discussed in our previous work [16], the epitaxial relation Al_2O_3 $\langle 1\,0\,0 \rangle$ // Fe_3O_4 $\langle -2\,1\,1 \rangle$ comes from the matching of the in-plane oxygen sub-lattice [10, 16]. In this case, the lattice constants of the in-plane oxygen triangular sub-lattices are approximately 2.92 Å and 2.85 Å for Al_2O_3 $(1\,0\,0)$ and Fe_3O_4 $(1\,1\,1)$ respectively [21, 22], which means a modest 2.5% mismatch. Since there is a 30° rotation between the *a*-axis of Al_2O_3 and that of the triangular oxygen sub-lattice in the basal plane Al_2O_3 $(0\,0\,1)$, to share the oxygen layer, the angle between the in-plane *a*-axis of Fe_3O_4 $(1\,1\,1)$ (Fe_3O_4 $\langle 0\,-1\,1 \rangle$), and that of the Al_2O_3 (Al_2O_3 $\langle 1\,0\,0 \rangle$) is expected to be 30° (or 90° considering the six-fold rotational symmetry), which is observed in figures 2(b) and (c).

---

[6] See supplementary material for more detailed information on x-ray diffraction, atomic force microscopy, and magnetometry.
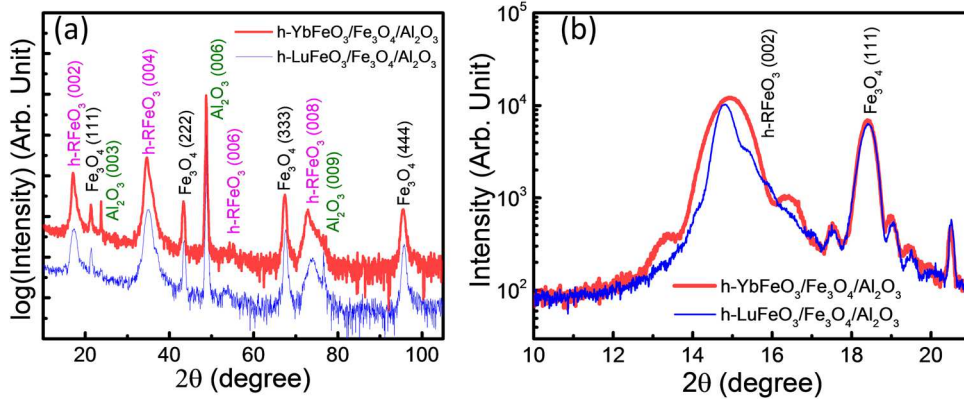
Figure 1. X-ray diffraction of the h-RFeO$_3$/Fe$_3$O$_4$/Al$_2$O$_3$ films. (a) Large-range $\theta - 2\theta$ scan using a cobalt K-α source ($\lambda = 1.79$ Å). (b) Small-range $\theta - 2\theta$ scan using a copper K-α source ($\lambda = 1.45$ Å). The ripples in the diffraction peaks are the Laue oscillations.
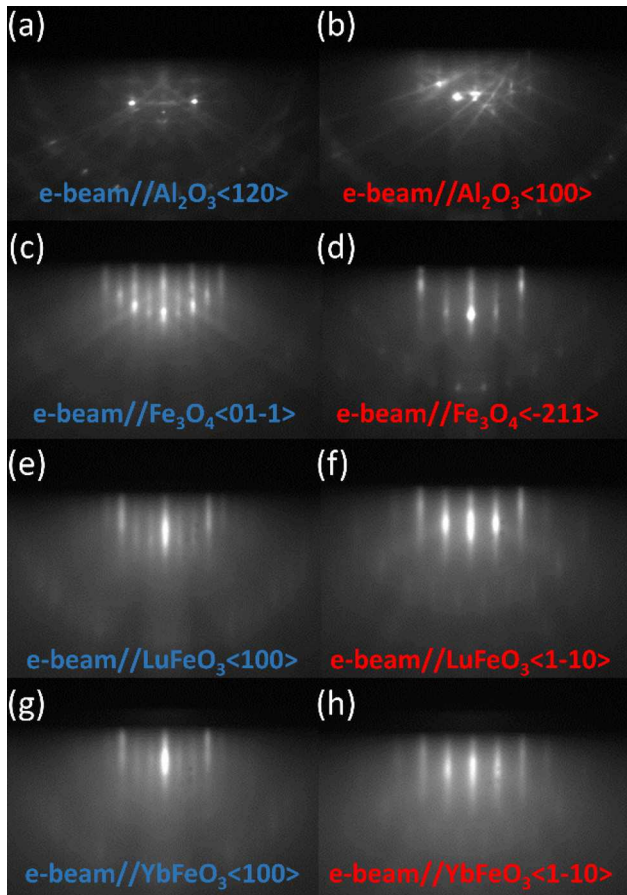

Figure 2. RHEED images of different surfaces with two perpendicular directions of incident electron beams relative to the substrate. In (a), (c), (e) and (g), the orientation of the substrate is fixed so that the electron beam is parallel to Al$_2$O$_3$ $\langle 1\,2\,0 \rangle$. In (b), (d), (f) and (h), the orientation of the substrate is fixed so that the electron beam is parallel to Al$_2$O$_3$ $\langle 1\,0\,0 \rangle$. The alignment between the electron beams and the films lattices are also indicated.

On the other hand, the matching of the oxygen sub-lattice between Fe$_3$O$_4$ (1 1 1) and h-RFeO$_3$ (0 0 1) is more complex, because the lattice constants of the in-plane oxygen triangular sub-lattices in h-RFeO$_3$ are approximately 3.45 Å, which is about 20% larger than that of the Al$_2$O$_3$ (0 0 1). Nevertheless, matching the Fe sub-lattices between Fe$_3$O$_4$ (1 1 1) and h-RFeO$_3$ (0 0 1) appears to be reasonable. As shown in the

side view of Fe$_3$O$_4$ (1 1 1) plane (figure 3(a)), there are two kinds of Fe layers that are parallel to the Fe$_3$O$_4$ (1 1 1) plane (figures 3(b) and (c)). For one of the layers in Fe$_3$O$_4$ (1 1 1) that is shown in figure 3(c), the in-plane lattice constant is 3.43 Å [22], which matches the in-plane Fe sub-lattice constant 3.44–3.45 Å in h-RFeO$_3$ (figures 3(d) and(e)) [7, 17] with a less than 1% difference. Therefore, the Fe$_3$O$_4$ (1 1 1) and h-RFeO$_3$ (0 0 1) could share the Fe sub-lattice on the interface, which leads to an epitaxial relation Fe$_3$O$_4$ $\langle 01 - 1 \rangle$// h-RFeO$_3$ $\langle 1\,0\,0 \rangle$, as shown in figures 2(c), (e) and (g).

The RHEED images in figures 2(e) and (g) show strong streaks separated by two weaker streaks, a pattern that is typical with a structural distortion with a propagation vector (1/3, 1/3, 0) [9]. In the case of h-RFeO$_3$, this structural distortion is the rotation of the FeO$_5$ trigonal bipyramid and the buckling of the LuO$_2$ layer (K$_3$ mode), which induces the displacements of the atoms along the c-axis (Γ_2^- mode), the ferroelectricity, and the canting of magnetic moments on Fe [9, 19, 23–25]. Therefore, it appears that the structural distortion that is critical for the multiferroicity in h-RFeO$_3$ is maintained in the h-RFeO$_3$/Fe$_3$O$_4$/Al$_2$O$_3$ films.

Next, we investigate the magnetic anisotropies of the h-YbFeO$_3$ (0 0 1)/Fe$_3$O$_4$ (1 1 1)/Al$_2$O$_3$ (0 0 1) films. For thin films, the magnetic anisotropy may come from the crystal structure (magneto-crystalline anisotropy) and from the dimension (shape anisotropy). The shape anisotropy is generated by the anisotropy of the depolarization factor in a film due to its quasi 2D shape. While the magneto-crystalline anisotropy depends on the specific crystal structure, for the shape anisotropy of a thin film, the hard axis is always along the out-of-plane direction. In the Fe$_3$O$_4$ films, the magneto-crystalline anisotropy is often dominated by those created by the anti-phase boundaries [26–28]. This type of anisotropy exists for all field directions, contributes little to the remanence and coercivity, and results in unsaturated magnetization up to 70 kOe [26–28]. For the Fe$_3$O$_4$ films, the shape anisotropy has a much smaller energy scale. Therefore, the two types of anisotropy are manifested in different field ranges. While the shape anisotropy governs the remanence and coercivity at the low field, the high field behavior of the magnetizations of the Fe$_3$O$_4$ films are determined by the magneto-crystalline anisotropy created by the anti-phase boundaries (see also the supplementary material).
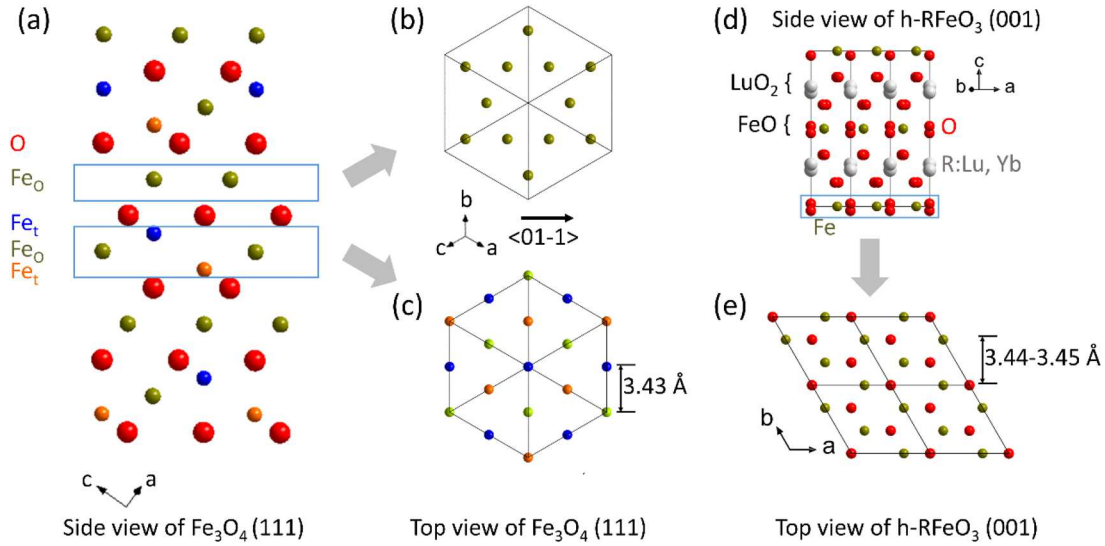
Figure 3. Structural model at the h-RFeO$_3$ (0 0 1)/Fe$_3$O$_4$ (1 1 1) interfaces. (a) Side view of the crystal structure of the Fe$_3$O$_4$ (1 1 1) film; the two kinds of Fe layers that are parallel to the Fe$_3$O$_4$ (1 1 1) plane are indicated by the boxes. Fe$_o$ and Fe$_t$ are Fe sites in oxygen octahedral and oxygen tetrahedral environments respectively. (b) and (c) are the top views of the two kinds of Fe layers indicated in (a). (d) Side view of the crystal structure of the h-RFeO$_3$ (0 0 1) film, where the FeO layer is indicated by the box. (e) Top view of the FeO layer in h-RFeO$_3$ (0 0 1) indicated in (d). (b)–(e) are in the same scale.
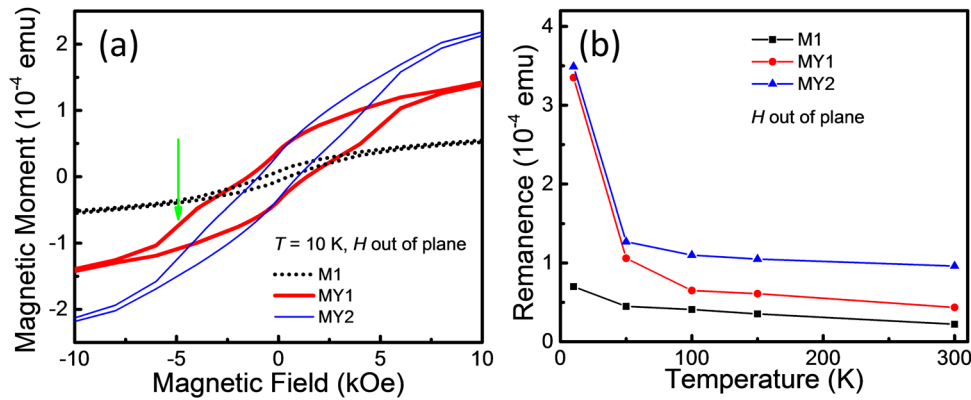
Figure 4. (a) Magnetic hysteresis loops for three film samples: Fe$_3$O$_4$ (8.5 nm)/Al$_2$O$_3$ (M1), h-YbFeO$_3$ (25 nm)/Fe$_3$O$_4$ (11 nm)/Al$_2$O$_3$ (MY1), h-YbFeO$_3$ (20 nm)/Fe$_3$O$_4$ (21 nm)/Al$_2$O$_3$ (MY2), measured at 10 K with magnetic field along the out-of-plane direction. (b) The magnetic remanence of the three film samples as a function of temperature.

For h-RFeO$_3$, the ferromagnetic order is parasitic to the antiferromagnetic order in which all the Fe moments lie in the basal plane [9]. The ferromagnetic magnetizations in h-RFeO$_3$ originate from the canting of the Fe moments toward the out-of-plane direction. The in-plane magnetization from Fe sites is symmetry forbidden. Therefore, in the h-RFeO$_3$ (0 0 1) films, the easy axis according to the magneto-crystalline anisotropy is along the out-of-plane direction and the shape anisotropy is not expected to play a role. In h-LuFeO$_3$, the saturation magnetization is small ($\approx$0.02 μ_B/f.u.) because it only comes from the magnetic canting on the Fe sites [9, 15]. In h-YbFeO$_3$, the paramagnetic Yb sites can be polarized by the exchange field of the Fe ferromagnetic magnetizations [8, 10], and contribute to the total magnetizations. Due to the paramagnetic nature of the Yb sites, this contribution is large at low temperature (~1 μ_B/f.u.) but drops rapidly at high temperature [10].

Figure 4(a) displays the magnetic hysteresis loops of a Fe$_3$O$_4$ (8.5 nm)/Al$_2$O$_3$ (0 0 1) (M1) film, an h-YbFeO$_3$ (25 nm)/ Fe$_3$O$_4$ (11 nm)/Al$_2$O$_3$ (MY1) film, and an h-YbFeO$_3$ (21 nm)/ Fe$_3$O$_4$ (20 nm)/Al$_2$O$_3$ (MY2) film at 10 K, with the magnetic field along the out-of-plane direction. The behavior of the M1 (Fe$_3$O$_4$) film is in line with a hard axis along the out of plane direction caused by the shape anisotropy (see also the supplementary material), as demonstrated by the small coercivity and magnetic remanence [16, 29].

The major features in the hysteresis loops in the h-YbFeO$_3$/ Fe$_3$O$_4$/Al$_2$O$_3$ films (MY1, MY2) in figure 4(a) can be understood in terms of the combined magnetization of the Fe$_3$O$_4$ layer and the h-YbFeO$_3$ layer, assuming that their corresponding magnetic anisotropies are preserved. According to the previous work, for a h-YbFeO$_3$ (0 0 1) film in an out-of-plane field, the magnetic remanence is more than half of the magnetization at 10 kOe [7, 8]. In contrast, for the Fe$_3$O$_4$ (1 1 1) film in an out-of-plane field, the magnetic remanence is much smaller (see figure 4(a)). Therefore, for both MY1 and MY2 films in an out-of-plane field, the magnetic remanence appears

to come mostly from the contribution of the h-YbFeO$_3$ layers (see figure 4(a)): by adding a h-YbFeO$_3$ layer on top a Fe$_3$O$_4$ layer (MY1 compared with M1), the magnetic remanence increases dramatically; in contrast, increasing the thickness of the Fe$_3$O$_4$ layer (MY2 compared with MY1) does not affect the magnetic remanence significantly; the boost of magnetic remanence in MY1 and MY2 compared with that in M1 (figure 4(b)), which is obtained by adding the h-YbFeO$_3$ layer, drops dramatically at 50 K and becomes much less significant when $T \geqslant 100$ K, consistent with the expected magnetic transition in h-YbFeO$_3$ above 120 K [8]. According to the previous work, for a h-YbFeO$_3$ (0 0 1) film in an out-of-plane field, the coercivity is in the range of 3–6 kOe [8], which can be identified from the step-like magnetization in MY1 (on top of the background of the gradual magnetization of Fe$_3$O$_4$) at about 5 kOe. For the film MY2, this step in the hysteresis loop is smeared because the Fe$_3$O$_4$ layer is thicker than that in MY1. These results suggest that the h-RFeO$_3$/Fe$_3$O$_4$ interfaces comprise two magnetic materials with different anisotropy; the out-of-plane direction is an easy axis for the h-RFeO$_3$ (0 0 1) layer but a hard axis for the Fe$_3$O$_4$ (1 1 1) layer (see also the supplementary material). Further investigations on the magnetic interactions between the Fe$_3$O$_4$ and h-YbFeO$_3$ layer may benefit from the element specific method in magnetic characterizations [30].

Conclusion

The epitaxial growth of h-RFeO$_3$ (0 0 1) films on Fe$_3$O$_4$ (1 1 1)/ Al$_2$O$_3$ (0 0 1) substrates has been demonstrated using pulsed laser depositions. The lattice constants and the epitaxial relations between h-RFeO$_3$ (0 0 1) and Fe$_3$O$_4$ (1 1 1), suggest a small mismatch at the interface. The h-RFeO$_3$ (0 0 1) crystal orientation at the interface, and the shape anisotropy in Fe$_3$O$_4$ (1 1 1), lead to the perpendicular alignment of magnetization at the h-RFeO$_3$ (0 0 1)/Fe$_3$O$_4$ (1 1 1) interface, which could be interesting in exploiting spintronic applications. Furthermore, the conductive nature of Fe$_3$O$_4$ will be beneficial in studying the multiferroicity of h-RFeO$_3$ in an electric field, especially the voltage controlled switch of magnetizations proposed by theory [25].

Acknowledgment

References

[1] Lines M E and Glass A M 1977 *Principles and Applications of Ferroelectrics and Related Materials* (Oxford: Clarendon)
[2] Tokura Y and Hwang H Y 2008 *Nat. Mater.* **7** 694
[3] Ramirez A P 1997 *J. Phys.: Condens. Matter* **9** 8171
[4] Zubko P, Gariglio S, Gabay M, Ghosez P and Triscone J-M 2011 *Annu. Rev. Condens. Matter Phys.* **2** 141
[5] Martin L W, Chu Y H and Ramesh R 2010 *Mater. Sci. Eng.* R **68** 89
[6] Feature N 2009 *Nature* **459** 28
[7] Iida H *et al* 2012 *J. Phys. Soc. Japan* **81** 24719
[8] Jeong Y K, Lee J, Ahn S, Song S-W, Jang H M, Choi H and Scott J F 2012 *J. Am. Chem. Soc.* **134** 1450
[9] Wang W *et al* 2013 *Phys. Rev. Lett.* **110** 237601
[10] Xu X and Wang W 2014 *Mod. Phys. Lett.* B **28** 1430008
[11] Spaldin N A, Cheong S W and Ramesh R 2010 *Phys. Today* **63** 38
[12] Schmid H 1994 *Ferroelectrics* **162** 317
[13] Disseler S M *et al* 2015 *Phys. Rev. Lett.* **114** 217602
[14] Cao S, Paudel T R, Sinha K, Jiang X, Wang W, Tsymbal E Y, Xu X and Dowben P A 2015 *J. Phys. Condens. Matter* **27** 175004
[15] Moyer J A, Misra R, Mundy J A, Brooks C M, Heron J T, Muller D A, Schlom D G and Schiffer P 2014 *APL Mater.* **2** 12106
[16] Zhang X, Yang S, Yang Z and Xu X 2016 *J. Appl. Phys.* **120** 85313
[17] Magome E, Moriyoshi C, Kuroiwa Y, Masuno A and Inoue H 2010 *Japan. J. Appl. Phys.* **49** 09ME06
[18] Wang W *et al* 2012 *Phys. Rev.* B **85** 155411
[19] Cao S *et al* 2016 *J. Phys.: Condens. Matter* **28** 156001
[20] Cao S, Zhang X, Sinha K, Wang W, Wang J, Dowben P A and Xu X 2016 *Appl. Phys. Lett.* **108** 202903
[21] Lewis J, Schwarzenbach D and Flack H D 1982 *Acta Crystallogr.* A **38** 733
[22] Finger L W, Hazen R M and Hofmeister A M 1986 *Phys. Chem. Miner.* **13** 215
[23] Fennie C J and Rabe K M 2005 *Phys. Rev.* B **72** 100103
[24] Wang H *et al* 2014 *Phys. Rev.* B **90** 14436
[25] Das H, Wysocki A L, Geng Y, Wu W and Fennie C J 2014 *Nat. Commun.* **5** 2998
[26] Margulies D T, Parker F T, Rudee M L, Spada F E, Chapman J N, Aitchison P R and Berkowitz A E 1997 *Phys. Rev. Lett.* **79** 5162
[27] Eerenstein W, Palstra T T M, Hibma T and Celotto S 2002 *Phys. Rev.* B **66** 201101
[28] Liu X H, Rata A D, Chang C F, Komarek A C and Tjeng L H 2014 *Phys. Rev.* B **90** 125142
[29] Della Torre E 1999 *Magnetic Hysteresis* (New York: IEEE Press)
[30] Stöhr J 1999 *J. Magn. Magn. Mater.* **200** 470